Available online at www.sciencedirect.com

SciVerse ScienceDirect

Ceramics International 39 (2013) S409–S413

CERAMICS INTERNATIONAL

www.elsevier.com/locate/ceramint

Crystal structure, microstructure and electrical properties of $(1-x-y)Bi_{0.5}Na_{0.5}TiO_3$–$xBi_{0.5}K_{0.5}TiO_3$–$yBiFeO_3$ ceramics near MPB prepared via the combustion technique

Rattiphorn Sumang[a,b], Naratip Vittayakorn[c], Theerachai Bongkarn[a,b,*]

[a]Department of Physics, Faculty of Science, Naresuan University, Phitsanulok 65000, Thailand
[b]Research Center for Academic Excellence in Petroleum, Petrochemicals and Advanced Materials, Naresuan University, Phitsanulok 65000, Thailand
[c]Department of Chemistry, Faculty of Science, King Mongkut's Institute of Technology Ladkrabang, Ladkrabang, Bangkok 10520, Thailand

Available online 16 October 2012

Abstract

$(1-x-y)Bi_{0.5}Na_{0.5}TiO_3$–$xBi_{0.5}K_{0.5}TiO_3$–$yBiFeO_3$ (BNKFT-x/y with $0.12 \le x \le 0.24$, $0 \le y \le 0.07$) lead-free piezoelectric ceramics have been prepared by the combustion technique. The effects of amounts of x and y on structures and electrical properties were examined. Powders and ceramics can be well calcined and sintered at 750 °C for 2 h and 1025–1050 °C, respectively. The results indicated that the crystalline structure and microstructure changed with the increase of x and y concentrations. XRD results of BNKFT-x/0.03 and BNKFT-0.18/y ceramics with $0.12 \le x \le 0.24$ and $0 \le y \le 0.07$ showed the rhombohedral–tetragonal morphotropic phase boundary (MPB). The addition of y caused a promoted grain growth while the addition of x suppressed the grain growth. The highest density ($\rho = 5.85$ g/cm^3), superior dielectric properties at T_c ($\varepsilon_r = 7846$ and $\tan\delta = 0.02$), remnant polarization measured at 40 kV/cm ($P_r = 20.1$ μC/cm^2) and piezoelectric coefficient ($d_{33} = 213$ pC/N) were obtained for $x = 0.18$ and $y = 0.03$.

Keywords: C. Dielectric properties; C. Ferroelectric properties; D. Perovskite; $(1-x-y)Bi_{0.5}Na_{0.5}TiO_3$–$xBi_{0.5}K_{0.5}TiO_3$–$yBiFeO_3$

1. Introduction

$Bi_{0.5}Na_{0.5}TiO_3$ (BNT), discovered by Smolenskii et al. [1] in 1960, is an ABO_3 type ferroelectric with perovskite phase. BNT is considered to be a promising candidate of lead-free piezoelectric ceramics with a relatively large remnant polarization ($P_r = 38$ μC/cm^2) and a high Curie temperature ($T_c = 320$ °C) [1]. However, pure BNT ceramic has high coercive field ($E_c = 73$ kV/cm), making the poling of the ceramics extremely difficult. In addition, pure BNT ceramic usually exhibits very poor piezoelectricity ($d_{33} = 58$ pC/N). To decrease the coercive field and improve the piezoelectric properties, a number of solid solutions of BNT with ABO_3-type ferroelectrics perovskite materials such as BNT–$Bi_{0.5}K_{0.5}TiO_3$ [2], BNT–$BaTiO_3$–$Bi_{0.5}K_{0.5}TiO_3$ [3] and BNT–$Bi_{0.5}K_{0.5}TiO_3$–$BiFeO_3$ [4] have been studied extensively. Among the solid solutions that have been developed so far, $(1-x-y)Bi_{0.5}Na_{0.5}TiO_3$–$xBi_{0.5}K_{0.5}TiO_3$–$yBiFeO_3$ (BNKFT-x/y) system near rhombohedral–tetragonal morphotropic phase boundary (MPB) has attracted considerable attention. The MPB compositions that showed remarkably superior electrical properties existed in the range of $0.18 \le x \le 0.21$ and $0 \le y \le 0.05$. Zhou et al. [5] reported that the optimum values of d_{33} and k_p are 170 pC/N and 36.6%, obtained from $0.79Bi_{0.5}Na_{0.5}TiO_3$–$0.18Bi_{0.5}K_{0.5}TiO_3$–$0.03BiFeO_3$ ceramics, respectively. Nevertheless, little is known about the dielectric and piezoelectric properties and there is no study on the ferroelectric properties.

Recently, in previous works we successfully fabricated high quality oxide ceramics such as $(Ba_{1-x}Sr_x)(Zr_xTi_{1-x})O_3$ [6] by the combustion technique. The advantages of this technique include inexpensive precursors and simple preparation process, and result in good electrical properties with low firing temperature and short dwelling

*Corresponding author at: Department of Physics, Faculty of Science, Naresuan University, Phitsanulok 65000, Thailand. Tel.: +66 55 963528; fax: +66 55 963501.
E-mail address: researchcmu@yahoo.com (T. Bongkarn).

0272-8842/$ - see front matter © 2012 Elsevier Ltd and Techna Group S.r.l. All rights reserved.
http://dx.doi.org/10.1016/j.ceramint.2012.10.104

time [7]. Thus, in this work, BNKFT-x/y ($0.12 \le x \le 0.24$ and $0 \le y \le 0.07$) ceramics were prepared by the combustion method. The effects of sintering temperature and the change of the x and y content on the phase formation, microstructure, and electrical properties of ceramics were investigated.

2. Experimental

BNKFT x/0.03 and BNKFT y/0.18 were prepared by the combustion technique. The starting materials used in this study were Bi_2O_3, Na_2CO_3, K_2CO_3, TiO_2 and Fe_2O_3. Stoichiometric amounts of starting powders were weighed and ball-milled using zirconia milling media for 24 h in ethanol. The raw materials were well-mixed with the fuel (glycine) in an agate mortar before calcination. The powders were calcined at 750 °C for 2 h and were mixed with polyvinyl alcohol; then it was pressed into discs with a diameter of 15 mm under 80 MPa. These pellets were subsequently sintered at 1000–1050 °C for 2 h.

Phase identifications of sintered ceramics were investigated using an XRD. The microstructures of all ceramics were observed using SEM. Dielectric properties were measured at a temperature in the range of 25–450 °C with a measured frequency of 1 kHz using a 4263B LCR-meter. Ferroelectric hysteresis loop was obtained using a ferroelectric test system. To obtain piezoelectric coefficient (d_{33}), the sintered pellets were polled under a DC field of 4 kV/mm at 120 °C in silicone oil for 30 min and measured using a quasistatic d_{33} meter.

3. Results and discussion

The XRD patterns of BNKFT-x/0.03 ceramics are shown in Fig. 1(a)–(c). All the samples exhibit a pure perovsktite structure, indicating that K^+ has diffused into the lattice to form a solid solution. In general, the rhombohedral structure is characterized by (003)/(021) peaks splitting between 39° and 41° and a single peak of (202) between 45° and 48°. Whereas a pure tetragonal structure is characterized by a single peak of (111) between 39° and 41° and (002)/(200) peaks splitting between 45° and 48°. For x=0.12, the (003)/(021) peaks' splitting occurs in the 2θ range of 39–41° (Fig. 1(b)) and the (202) peak is asymmetric in the range of 45–48° (Fig. 1(c)). When x content is increased, the (003)/(021) peak begins to merge into a single (111) peak and the (202) peak starts to split into two peaks of (002)/(200), which reveal that the crystalline structure has two phases between rhombohedral and tetragonal coexisting. Furthermore, the increasing x content is affected by the increase of the tetragonal and decrease of the rhombohedral phases.

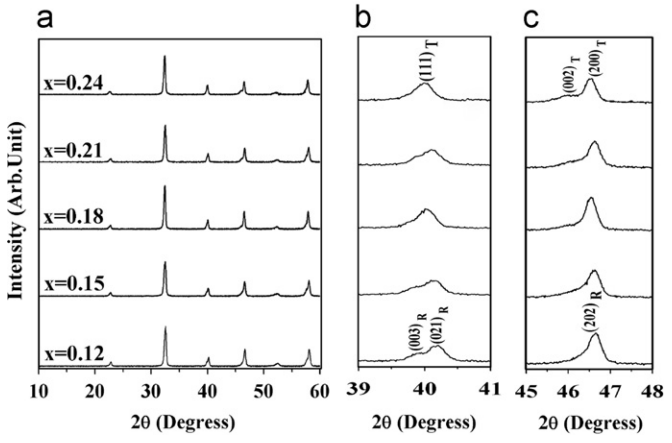

Fig. 1. X-ray diffraction patterns of BN KFT-x/0.03 sintered ceramics in the 2θ range of (a) 10°–60°, (b) 39°–41° and (c) 45°–48°.

The SEM micrographs of BNKFT-x/0.03 ceramics are shown in Fig. 2(a)–(c). All ceramics show a quasi-cubic morphology with clear grain boundaries. The average grain size decreases from 2.67 μm to 0.98 μm when the x content is increased from 0.12 to 0.24, as listed in Table 1. The grains become evidently smaller with increasing x content, which can be explained by the fact that the K^+ ion which concentrates near the grain boundaries has substantially reduced mobility as densification occurred [5]. The decrease in the mobility of the grain boundary weakens the mass transport. As a result, grain growth is obviously inhibited and smaller grains are formed in the ceramic samples at a high concentration of x [5]. The measured density and relative density of the BNKFT-x/0.03 ceramics with different x contents are listed in Table 1. The density increases and reaches a maximum value of 5.85 g/cm^3 or ~96.6% of the theoretical density obtained from the sample with x=0.18, and it slightly decreases with $x > 0.18$ (Table 1).

Fig. 3(a) shows the temperature dependences of the dielectric constant (ε_r) of BNKFT-x/0.03 ceramics which were measured at 1 kHz. The dielectric constant showed two peaks (T_d at low temperature and T_c at high temperature) in all samples. T_d is the temperature at which the phase transition from ferroelectric (rhombohedral) to anti-ferroelectric (tetragonal) occurred. T_c is the temperature at which the transition from anti-ferroelectric (tetragonal) to paraelectric (cubic) occurred. When there was an increase of x, T_d of the sample shifted to the lower temperature from 185 °C to 94 °C whereas T_c shifts to higher temperature regions from 282 °C to 321 °C, as listed in Table 1. At Curie temperature, the maximum dielectric constant was observed in all samples. It tends to increase from 5890 to 7850 when the x content increases from 0.12 to 0.18. On further increasing x content to 0.24, ε_r decreases to 3750, as listed in Table 1. The dielectric loss at T_c tends to decrease from 0.04 to 0.02 when the x content increases from 0.12 to 0.24, as shown in Table 1.

The ferroelectric polarization–electric field (P–E) loop of BNKFT-x/0.03 ceramics measured at 40 kV/cm is shown in Fig. 4(a). For the compositions with x=0.12 and x=0.15, the P–E loops were not fully saturated. As x increased, the loops became relatively saturated. The measured remnant polarization (P_r) of BNKFT-x/0.03

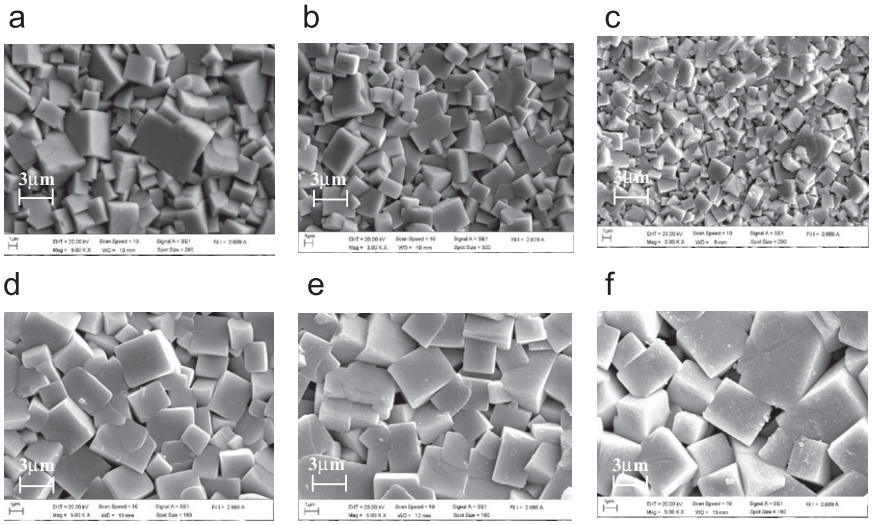

Fig. 2. SEM images of BNKFT-x/y sintered ceramics with (a) $x=0.12$, (b) $x=0.18$, (c) $x=0.21$, (d) $y=0$, (e) $y=0.03$ and (f) $y=0.07$.

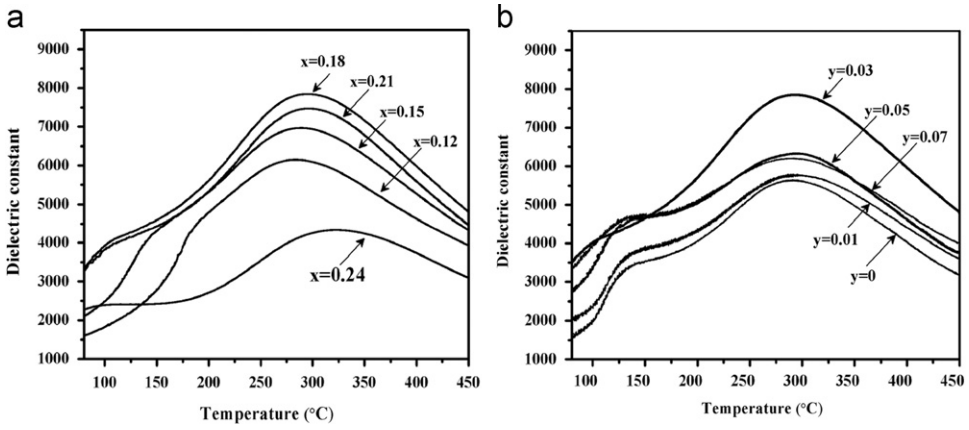

Fig. 3. The temperature dependences of dielectric constant (ε_r) of the (a) BNKFT-x/0.03 and (b) BNKFT-0.18/y ceramics.

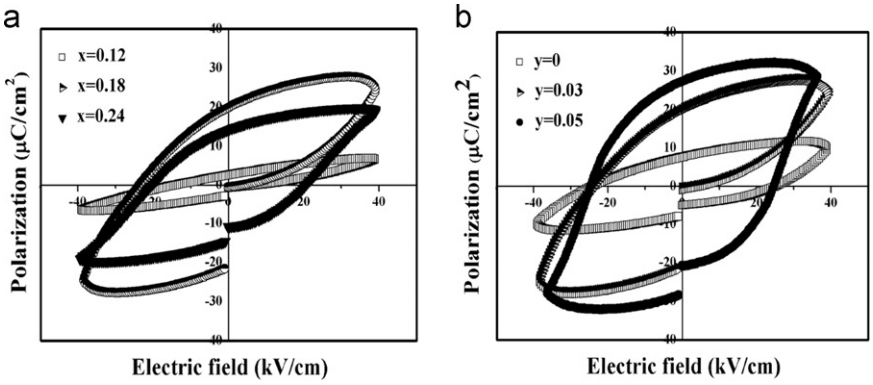

Fig. 4. Ferroelectric hysteresis loops of (a) BNKFT-x/0.03 and (b) BNKFT-0.18/y ceramics.

ceramics increases from 2.7 μC/cm^2 to the maximum value (20.1 μC/cm^2) at $x=0.18$, and then drops to 13.3 μC/cm^2 with a further increase of x to 0.24. The decrease in P_r as x content increases suggests that the high substitutions of K^+ ions for Na^+ ions would cause the decrease in relative displacement of unit cells. The coercive field (E_c) continuously increases from 13.2 kV/cm to 23.2 kV/cm when the content of x increases from 0.12 to 0.18. This result may be due to the possible index of domain reorientation and rotation is gradually hindered as x content increases [8]. With a further increase in the x content to 0.24, E_c tends to decrease to 21.3 kV/cm, as listed in Table 1. The

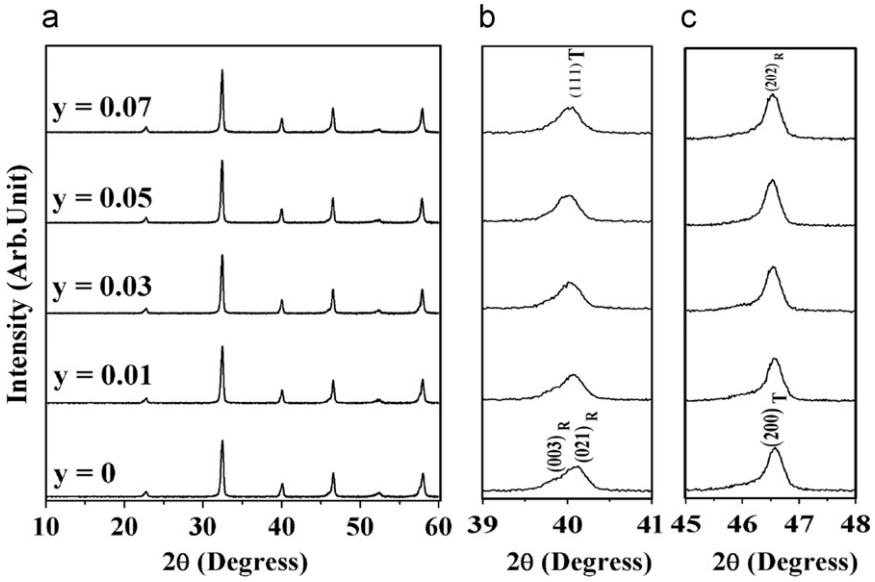

Fig. 5. X-ray diffraction patterns of BNKFT-0.18/y sintered ceramics.

piezoelectric coefficients of BNKFT-x/0.03 ceramics are illustrated in Table 1. The piezoelectric coefficients d_{33} of all ceramics first increases and then decreases with increasing x content. The maximum d_{33} is obtained at $x=0.18$, which is 213 pC/N. The decrease of d_{33} is due to the clamping effect associated with oxygen vacancies hindering sufficient reorientation of ferroelectric domains during electrical poling [8]. The d_{33} at $x=0.18$ is higher than that of the previous work [9].

The optimum value of x content was fixed at 0.18, and then y was varied from 0 to 0.07. The XRD patterns of BNKFT-0.18/y ceramics are shown in Fig. 5(a)–(c). All samples show the pure perovskite structure (Fig. 5(a)). For $y=0$, in the 2θ range of 39–41°, the (003)/(021) peaks' splitting is slight (Fig. 5(b)). The peak splitting diminishes and begins to merge into a single (111) peak with increasing y content from 0 to 0.07. Moreover, in the 2θ range of 45–48° for $y=0$, the peak is asymmetric (Fig. 5(c)). When there is an increase of y content, the peak becomes more asymmetric and skews to the left side. These results indicate a coexistence between tetragonal and rhombohedral phases in the ceramics. The structures are in good agreement with the previous work [5].

The SEM photomicrograph of BNKFT-0.18/y sintered pellets are shown in Fig. 2(d)–(f). It can be seen that the grain exhibits an almost quasi-cubic morphology. The average grain size increased from 2.15 μm to 2.81 μm with increasing y content (Table 1). The increased grain size of the ceramics is due to the Fe^{3+} entering into the sixfold coordinated B-site to substitute for Ti^{4+} because of radius matching [8]. The densities of BNKFT-0.18/y ceramics with different y contents are listed in Table 1. The density increases from 5.57 g/cm^3 to 5.85 g/cm^3 (93.1–96.4% of theoretical density) when concentration of x increases from 0 to 0.03, and then drops to 5.77 g/cm^3 (93.9% of theoretical one) with further increasing of y to 0.07.

Temperature dependence of the dielectric constant (ε_r) of BNKFT-0.18/y ceramics measured at 1 kHz is shown in Fig. 3(b). Two abnormal temperature peaks exist for all samples with different compositions. The T_d and T_c shift to lower temperature regions from 131 °C to 123 °C and 294 °C to 282 °C, respectively, with increasing y content from 0 to 0.07, as listed in Table 1. The results agree with the results of Zhou et al. [5]. At T_c, the maximum dielectric constant tends to increase in value from 5630 to 7850 when the y content increased from 0 to 0.03. After that, the maximum dielectric constant of ceramics decreases as the concentration of y increases above 0.03, as listed in Table 1. The dielectric loss at T_c tends to increase from 0.02 to 0.04 when the y content increases from 0 to 0.07, as shown in Table 1. ε_r and tan δ at T_c (at 1 kHz) of all compositions are closely consistent with the results of previous work [5].

The ferroelectric polarization–electric field (P–E) loop of BNKFT-0.18/y ceramics is shown in Fig. 4(b). When the y content increases from 0 to 0.07, the P–E loops tend to be not fully saturated. The value of P_r is found to increase from 7.6 μC/cm^2 to 27.5 μC/cm^2 with increasing y content from 0 to 0.05. With a further increase in y content to 0.07, P_r decreases to 15.0 μC/cm^2, as listed in Table 1. The decreasing trend of E_c shows the minimum value at $y=0.03$. With a further increase of y content to 0.07, E_c increases to 29.4 kV/cm, as listed in Table 1. The piezoelectric coefficient of BNKFT-0.18/y ceramics is listed in Table 1. When $y=0$, the piezoelectric coefficient d_{33} is 164 pC/N. With increasing content of y, d_{33} reaches the maximum value of 213 pC/N at $y=0.03$, and then drops in value.

4. Conclusion

Lead free BNKFT ceramics were synthesized by the combustion technique. The variations of x and y contents directly affect the crystal structure, microstructure, density,

Table 1
Average grain size, density, dielectric constant (ε_r), dielectric loss (tanδ), depolarization and Curie temperature (T_d and T_c), remnant polarization (P_r), coercive field (E_c), and piezoelectric coefficient (d_{33}) of BNKFT-x/y ceramics.

Composition	Average grain size (μm)	Measured density (g/cm^3)	Relative density (%)	ε_r at T_c	tan δ at T_c	T_d (°C)	T_c (°C)	P_r (μC/cm^2)	E_c (kV/cm)	d_{33} (pC/N)
x=0.12	2.67	5.73	94.6	5890	0.04	185	282	2.7	13.2	75
x=0.15	2.41	5.79	95.7	6970	0.03	147	299	4.6	14.2	103
x=0.18	2.39	5.85	96.6	7850	0.02	117	302	20.1	23.2	213
x=0.21	1.33	5.79	94.1	7310	0.02	115	312	19.3	16.3	39
x=0.24	0.98	5.57	92.1	3750	0.02	94	321	13.3	21.3	37
y=0	2.15	5.57	93.1	5630	0.02	131	294	7.6	25.2	164
y=0.01	2.23	5.63	93.8	5640	0.02	129	291	19.9	27.0	195
y=0.03	2.44	5.85	96.4	7850	0.02	110	287	20.1	23.2	213
y=0.05	2.73	5.80	95.1	6330	0.03	125	285	27.5	24.4	195
y=0.07	2.81	5.77	93.9	6320	0.04	123	282	15.0	29.4	95

dielectric, ferroelectric and piezoelectric properties of the BNKFT-x/0.03 and BNKFT-0.18/y ceramics. The XRD indicated that the ceramics possess pure single phase of perovskite structure, indicating that K^+ and Fe^+ have diffused into the lattice. With increasing x and y contents, grain size decreases and increases, respectively. The optimum electric properties can be obtained at x=0.18 and y=0.03, as follows: ρ=5.85 g/cm^3, ε_r=7850, tan δ=0.02, P_r=20.1 μC/cm^2 (measured at 40 kV/cm) and d_{33}=213 pC/N. With superior electric properties, this work indicates that the BNKFT-x/y ceramics prepared by the combustion technique are better than the BNKFT-x/y ceramics prepared by solid state.

Acknowledgments

This work was financially supported by the Thailand Research Fund through the Royal Golden Jubilee Ph.D. Program (Grant no. PHD/0213/2552) to Miss Rattiphorn Sumang and Assist. Prof. Dr. Theerachai Bongkarn. The authors wish to thank the Naresuan University for supporting facilities. Thanks are given to Dr. Antony Harfield for his help in editing the manuscript.

References

[1] G.A. Smolenskii, V.A. Isupov, A.I. Agranovskaya, N.N. Krainik, New ferroelectrics of complex composition IV, Soviet Physics Solid State 2 (11) (1961) 2651–2654.
[2] L. Gao, Y. Huang, Y. Hu, H. Du, Dielectric and ferroelectric properties of $(1-x)BaTiO_3$–$xBi_{0.5}Na_{0.5}TiO_3$ ceramics, Ceramics International 33 (2007) 1041–1046.
[3] S.T. Zhang, B. Yang, W. Cao, The temperature-dependent electrical properties of $Bi_{0.5}Na_{0.5}TiO_3$–$BaTiO_3$–$Bi_{0.5}K_{0.5}TiO_3$ near the morphotropic phase boundary, Acta Materialia 60 (2012) 469–475.
[4] C.R. Zhou, X. Liu, W. Li, C. Yuan, Structure and piezoelectric properties of $Bi_{0.5}Na_{0.5}TiO_3$–$Bi_{0.5}K_{0.5}TiO_3$–$BiFeO_3$ lead-free piezoelectric ceramics, Materials Chemistry and Physics 114 (2009) 832–836.
[5] C.R. Zhou, X.Y. Liu, W.Z. Li, C.L. Yuan, Dielectric relaxor behavior of A-site complex ferroelectrics of $Bi_{0.5}Na_{0.5}TiO_3$–$Bi_{0.5}K_{0.5}TiO_3$–$BiFeO_3$, Solid State Communications 149 (2009) 481–485.
[6] A. Thongtha, K. Angsukased, T. Bongkarn, Fabrication of $(Ba_{-1-x}Sr_x)(Zr_xTi_{1-x})O_3$ ceramics prepared using the combustion technique, Smart Materials and Structures 19 (2010) 124001.
[7] R. Pampuch, Advanced HT ceramic materials via solid combustion, Journal of the European Ceramic Society 19 (1999) 2395–2404.
[8] L. Gao, H. Yanqiu, Y. Hu, H. Du, Dielectric and ferroelectric properties of $(1-x)BaTiO_3$–$xBi_{0.5}Na_{0.5}TiO_3$ ceramics, Ceramics International 33 (2007) 1041–1046.
[9] M. Zou, H. Fan, L. Chen, W. Yang, Microstructure and electrical properties of $(1-x)[0.82Bi_{0.5}Na_{0.5}TiO_3$–$0.18Bi_{0.5}K_{0.5}TiO_3]$–$xBiFeO_3$ lead-free piezoelectric ceramics, Journal of Alloys and Compounds 495 (2010) 280–283.